APCC
APEC CLIMATE CENTER

TECHNICAL REPORT

APCC
APEC CLIMATE CENTER

PREFACE

It is our pleasure to present to you the APEC Climate Center (APCC)'s Technical Report 2011, which reports the core outcomes of our research activities from the past year.

Since 2005, APCC, as a hub of climate information in the Asia-Pacific region, has strived to share our analysis and prediction of abnormal climate and to apply this information to regional development. The center has established the largest Multi-Model Ensemble (MME) system for seasonal prediction through its international science network and has provided value-added products to various stakeholders. Recently, APCC has expanded its mandate to include enhancement of the capacity of APEC member economies information to respond effectively to climate change and variability through better application of climate.

To achieve its research and social objectives, in 2011, APCC made efforts to research improvements in its climate prediction performance from various angles and towards better understanding of climate variability and the reproducibility of the climate models for the relevant application of climate information to society. The following technical report provides more information about our research outcomes from 2011.

APCC will continue to improve the quality and accuracy of climate information, recognizing that the utility of this information is only as good as its quality. We would like to make the best use of our research results for the benefit of society and academia. We also welcome any feedback on this report or on our services.

My best and warmest regards to all of you.

Dr. Chin-Seung Chung
Director/APEC Climate Center

CONTENTS

Interannual Variability of the Western North Pacific Summer Monsoon in APEC Climate Center Multi-Model Ensemble

Dr. Bong-Geun Song

APCC
TECHNICAL REPORT 2011-01

Interannual Variability of the Western North Pacific Summer Monsoon in APEC Climate Center Multi-Model Ensemble

Dr. Bong-Geun Song

ABSTRACT

Most state-of-the-art general circulation models (GCMs) are unable to predict well the year-to-year variation in the western North Pacific summer monsoon (WNPSM). Good skill is unrealized as model biases distort the distribution of the predicted monsoon rainfall in individual models, despite the fact that the wind fields are relatively well reproduced. However, a multi-model ensemble (MME) approach can considerably reduce biases of rainfall simulations. Here we demonstrate that, by using combinations of hindcast runs from thirteen different models participating in the APEC Climate Center (APCC) MME forecasts, the WNPSM rainfall can be skillfully predicted. It is also found that the coupled MME (CMME) mean predictions which comprise Tier-1 prediction systems outperform each individual model in capturing both the spatial and temporal variability of WNPSM circulation.

1. INTRODUCTION

The western north Pacific (WNP) summer monsoon (WNPSM) and the East Asian summer monsoon (EASM) are linked parts of the global climate system that are affected by the El Niño-Southern Oscillation (ENSO) and sea surface temperature variations in the western Pacific and surrounding oceans, the tropospheric biennial oscillation, and the South Asian summer monsoon (Yasunari 1990, Chang and Li 2000, Wang et al. 2001). In addition, typhoons in the WNP may be considered to be an impactful component of the EASM for their contribution of substantial amounts of rainfall to the region. The WNPSM has been a challenging subject in the research and prediction fields due to its links with other cyclical components of the climate system. The WNPSM exhibits year-to-year variability but also impacts the climate system on longer timescales due to its contribution to the EASM and ENSO. In particular, the prediction of rainfall over the WNP has been regarded as a major factor in the development of improved global circulation models (GCMs) for monsoon prediction. Predicting the variation of the Asian monsoon using GCMs is one of the most challenging tasks in dynamical seasonal prediction. Many atmospheric GCMs (AGCMs), which are employed for climate forecasts in a number of operational centers, are poorly equipped to predict monsoon rainfall (Kang et al. 2002; Wang et al. 2004; Kang and Shukla 2005). This poor performance can be attributed to monsoon biases

in the dynamical models, as monsoon simulations are known to be sensitive to physical parameterizations as well as model resolution (Sumi et al. 2005). Wang et al. (2004) suggested that the poor performance of AGCM-based simulations of precipitation over the western Pacific is due to the tier-2 prediction system, in which atmospheric behavior is forced by prescribed SSTs. In nature, however, the ocean-atmosphere coupled processes are active and atmospheric feedback to the ocean, which is absent from the tier-2 approach, is important in the western Pacific. Wang et al. (2005) also suggested that the lack of consideration of air-sea coupling in tier-2 climate prediction systems could be another source of error in the prediction of Asian monsoon variability.

In order to quantify the variability of the Indian summer monsoon (ISM) and WNPSM, Wang et al. (2001) defined the ISM index and WNP monsoon index (WNPMI) originally proposed by Wang and Fan (1999). They contrasted features of the ISM and WNPSM and found that the monsoons abate during El-Niño development and decay, respectively. Previous studies have also suggested the importance of understanding the WNPSM variability and its interaction with ENSO (Wu and Wang 2000, Wang et al. 1999, Wang et al. 2000). Using simple monsoon indices to investigate monsoon variability can aid the objective assessment of the capability of GCMs in predicting and reproducing monsoon variability.

The potential of multi-model ensemble (MME) techniques in improving dynamical seasonal predictions has been examined in a number of recent studies (Krishnamurti et al. 2000; Barnston et al. 2003). MME seasonal forecasts based on either a simple composite or an optimally weighted ensemble of individual model outputs are shown to have superior skill compared to single model predictions. The better performance of the MME predictions is generally understood to result from better quantification of model bias uncertainty. Based on the results of multi-institutional joint research efforts such as the Development of a European Multimodel Ensemble Prediction System for Seasonal to Interannual Prediction (DEMETER) and the APEC Climate Center/Climate Prediction and its Application to Society (APCC/CliPAS) projects (Palmer et al. 2004; Wang et al., 2008), operational centers such as the European Center for Medium-Range Weather Forecasts (ECMWF), APCC and the International

Research Institute (IRI) have begun to issue MME seasonal climate predictions.

This study examines the seasonal predictability of the western north Pacific summer monsoon (WNPSM), which displays pronounced interannual variability (Tanaka 1997, Wang etal. 1999, 2001, Wu and Wang 2000, Chou et al. 2003). The variability of the WNPSM has profound impacts on the boreal summer Asian climate, including rainfall over the Philippine Sea and the behavior of the Meiyu-Changma-Baiu rainband (see Wang et al. 2001 and reference therein). We assess the predictability of the WNPSM based on retrospective forecasts from models component to the APCC MME seasonal prediction system. In these numerical experiments, no future information is used after the models are initialized (see Section 2 on experimental setup). Our results, therefore, can be seen as an assessment of the predictability of the WNPSM as based on real climate forecasts. The focus is on the efficacy of the MME approach in capturing the spatial-temporal variability of the WNPSM. Our findings demonstrate that the MME approach can overcome the deficiencies of WNPSM simulations. In particular, the MME technique results in a pronounced improvement in the monsoon rainfall prediction relative to that achieved by the single model approach.

2. METHODOLOGY

2.1 Data

In this study, thirteen hindcast experiments based on dynamical models participating in the APCC MME seasonal predictions are examined. A simple description of the models is given in Table 1. BCC, JMA, NCEP, PUN and POAMA are Tier-1 coupled prediction systems (coupled GCMs, CGCMs), each of which includes 5~10 ensemble members from different initial conditions that span each month. For other hindcast experiments, Tier-2 systems are used in which AGCMs are forced with either observed or predicted sea surface temperature (SST) anomalies prescribed in the lower boundary, and all ensemble members of each model are started from different

atmospheric initial conditions that span each month before the hindcast month. Each hindcast dataset spans the common period of 1983-2003 and includes precipitation and the wind component at 850 hPa. The observational datasets used for comparison are based on the Climate Anomaly Monitoring System (CAMS) and ORL Precipitation Index (OPI) (Janowiak and Xie, 1999), upper-air wind fields from the National Centers for Environmental Prediction (NCEP)-Department of Energy (DOE) reanalysis 2 (Kanamitsu et al., 2002) and OISST.

Table 1 Description of the thirteen models used in this study.

Acronym	Organization	Model Resolution	Hindcast Type	SST Boundary Condition	No. of Ensemble Members
BCC	Beijing Climate Center / China	T63L16	SMIP	Predicted SST	8
CWB	Central Weather Bureau / Chinese Taipei	T42L18	SMIP	Observed SST	10
GCPS	Seoul National University / Korea	T63L21	SMIP/HFP	Predicted SST	4
GDAPS_F	Korea Meteorological Administration / Korea	T106L21	SMIP/HFP	Predicted SST	20
JMA	Japan Meteorological Agency / Japan	T95L40	HFP	Predicted SST	5
MSC_GEM	Meteorological Service of Canada / Canada	2° L50	SMIP2/HFP	Persistent SST	10
MSC_GM2	Meteorological Service of Canada / Canada	T32L10	SMIP2/HFP	Persistent SST	10
MSC_GM3	Meteorological Service of Canada / Canada	T63L32	SMIP2/HFP	Persistent SST	10
MSC_SEF	Meteorological Service of Canada / Canada	T95L27	SMIP2/HFP	Persistent SST	10
NCEP	National Centers for Environmental Prediction / USA	T62L64	CMIP	Predicted SST	15
NIMR	National Institute of Meteorological Research / Korea	4°×5° L17	SMIP/HFP	Observed SST	10
PNU	Pusan National University / Korea	T42L18	CMIP	Predicted SST	5
POAMA	Centre for Australian Weather and Climate Research / Bureau of Meteorology / Australia	T63L21	CMIP	Predicted SST	10

2.2 Methods

The simple composite method (SCM) is used to produce the MME hindcast products from the GCMs' hindcast datasets for the period of 1983-2003. The MME method is considered to be an efficient solution to improve weather and climate forecasts. The basic purpose of MME is to avoid inherent model error by using a number of independent and skillful models to attain better coverage of the complete range of possible climate phase spaces. The SCM is a deterministic forecast scheme that computes a simple arithmetic mean of the predictions of individual member models. The SCM is based on the assumption that each model is relatively independent and can, to some extent, forecast the regional climate well, so that an accurate forecast can be achieved by a simple composite of the predictions from the component models. This scheme maintains the dynamics of each component model due to the simple spatial filtering for each variable at each grid point. Accordingly, this scheme retains the common advantages and limitations of the component models' predictions. Therefore, the SCM results are effectively a combination of the component models' hindcast anomalies. Skill improvements result from the reduction of climate noise by ensemble averaging. In this scheme, the ensemble mean assigns the same weight of 1/N to each of the N member models regardless of its relative performance.

To investigate the WNPSM circulation and its predictability, we have performed a multivariate empirical orthogonal function (EOF) and correlation analysis. The analysis domain of the multivariate EOF is the western Pacific monsoon region (5-45°N, 100-170°E). To quantify the interannual variability of the summer monsoon variability in the WNP region, we used the WNPMI proposed by Wang et al. (2001), which is defined by the meridional difference between zonal winds at 850 hPa averaged over a southern rectangular region (5°N-15°N, 100°E-130°E) and a northern rectangular region (20°N-30°N, 110°E-140°E) (see Fig. 1).

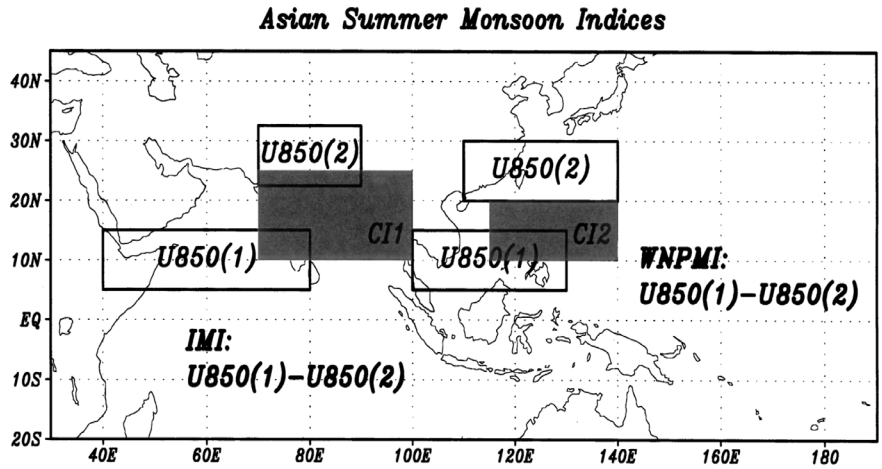

Figure 1 Schematic diagram for the definition of the monsoon circulation indices, IMI and WNPMI. Shaded boxes indicate the regions of rainfall indices, CI1 and CI2. The solid boxes denote regions where the zonal winds are used to define the monsoon circulation indices (Wang et al., 2001).

According to Wang et al. (2001), the main features of the dominant mode during a strong WNPSM in the WNP-EASM region are an anomalous cyclone elongated along 20°N, which dictates the WNP, and westerly and easterly anomalies that prevail between 5° and 15°N, and 20°N and 30°N, respectively (Fig. 2a). An anomalous anticyclonic ridge extends from the central Pacific to eastern China and Japan around 35°N. The WNPMI is highly correlated with the principal component of the dominant EOF pattern of the 850 hPa wind anomalies in the WNP monsoon domain. Thus, the index represents the dominant modes of interannual variations of the WNPSM, which reflect the variations in vorticity of the low-level monsoon flows, and it measures the variability of the WNP monsoon trough and the subtropical ridge, as well as the Philippine Sea convection.

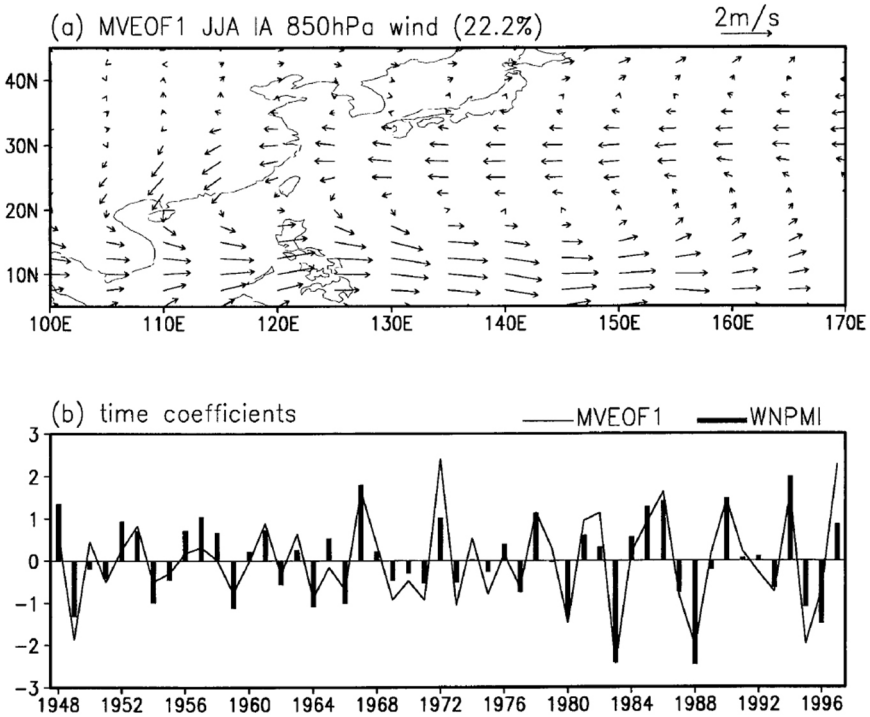

Figure 2 (a) The leading multivariate EOF mode and (b) time coefficient of 850-hPa winds in the western North Pacific-east Asian monsoon region for the summers of 1948–97. The wind scales are displayed at the upper-right corners of (a) and (b). For comparison, the normalized WNPMI is plotted in (b) using bar charts (Wang et al., 2001).

3. RESULTS

3.1 JJA mean fields of 850 hPa wind and precipitation in the WNP-EA region

We first compare the observed and model-simulated circulation climatologies over the western Pacific monsoon region. Figure 3 gives the mean values of JJA precipitation and 850 hPa wind for the observed data and model hindcasts. The observations show heavy monsoon rainfall during the boreal summer over Indochina, the South China and Philippine Seas region, the western Pacific (WNSP region between 5°N-20°N and 100°E-150°E), as well as over the Korean peninsula and southern

part of Japan (EASM region between 20°N-40°N and 100°E-140°E) (Fig. 3a). Over the western North Pacific, a confluence of three low-level wind branches, namely the strong westerlies from Southeast Asia, the cross-equatorial flow near the Philippines and the easterly flow associated with the subtropical high, can be discerned. Inspection of the hindcast simulations reveals that many models have difficulty reproducing specific aspects of the observed monsoon circulation pattern (Fig. 3b-n). In particular, GCPS, JMA, MSC_GM3, NCEP and PNU simulations of the western Pacific monsoon circulation are mostly comparable with the observed pattern, except that all show monsoon troughs that are stronger than the observed trough. On the other hand, the monsoon westerlies modeled by the MSC_GEM, MSC_GM2 and POAMA are too strong and are displaced eastward compared to those observed. The BCC, CWB, GDAPS_F, MSC_SEF and NIMR do not penetrate far enough in the western Pacific, thus they underestimate precipitation near the Philippines.

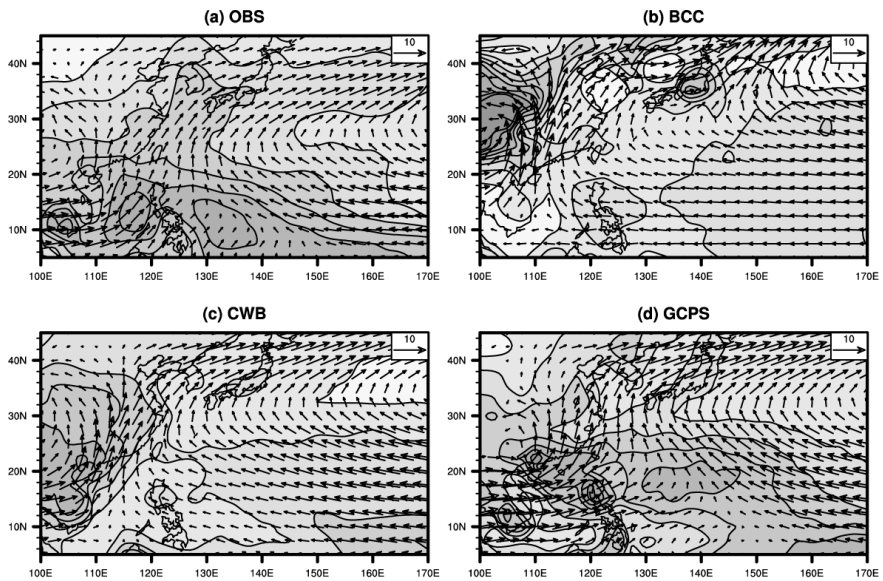

Figure 3 Mean fields of 850 hPa wind (vectors, see scale at upper right of each panel; units: ms^{-1}) and precipitation (shading, see scale bar at bottom; units: mm/day) based on (a) observations and (b) BCC, (c) CWB, (d) GCPS, (e) GDAPS_F, (f) JMA, (g) MSC_GEM, (h) MSC_GM2, (i) MSC_GM3, (j) MSC_SEF, (k) NCEP, (l) NIMR, (m) PNU and (n) POAMA for the JJA season of 1983-2003..

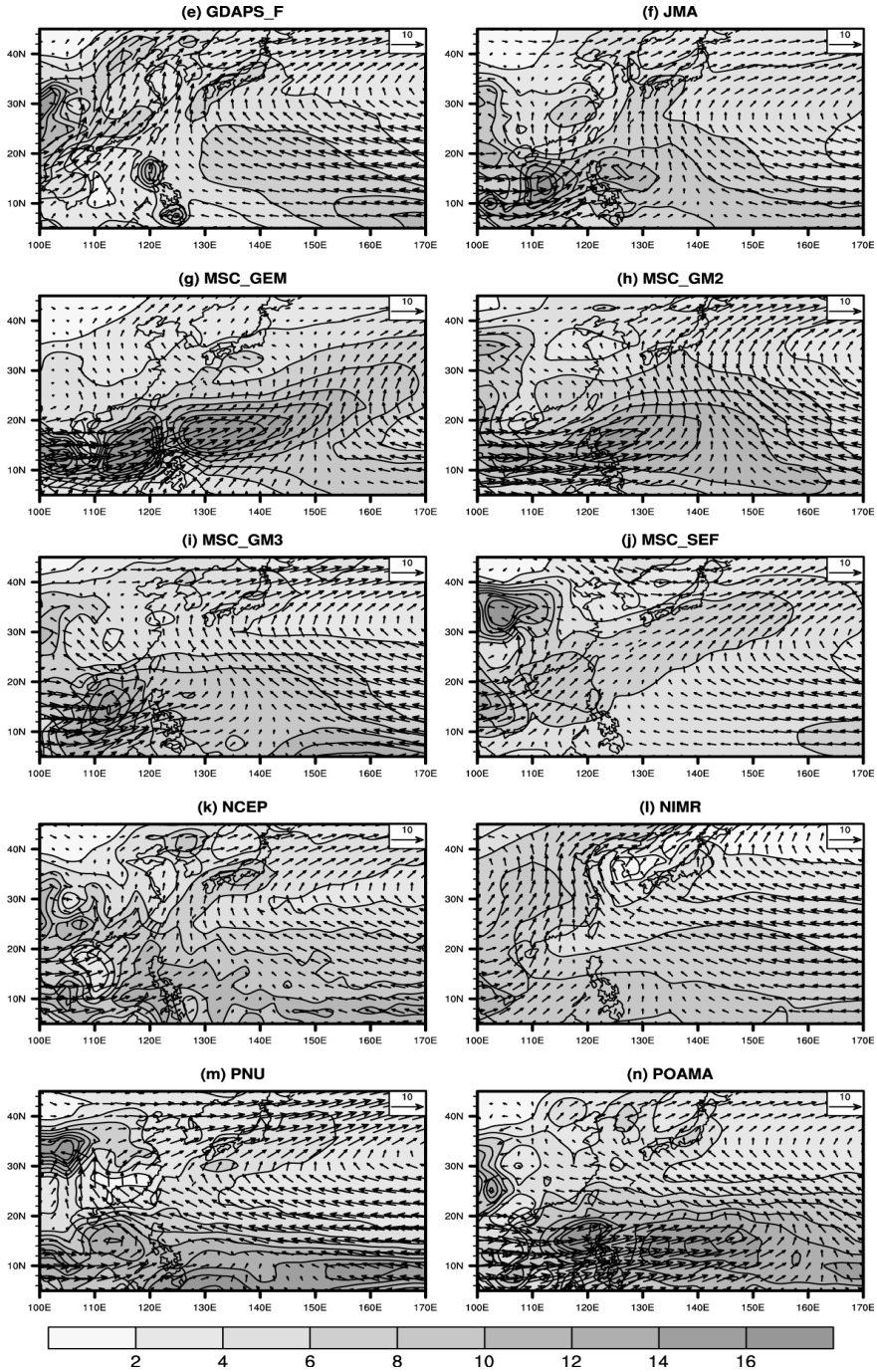

Figure 3 Continued.

Table 2 shows the pattern correlations between observations and GCM-simulated circulation anomalies for the JJA period. The monsoon circulations of GCPS, JMA, MSC_GM2, MSC_GM3, NCEP, and PNU are relatively well simulated compared to other models. The correlation values of the low-level westerlies and precipitation in the JMA, MSC_GM3, NCEP and PNU simulations are more than 0.86 and 0.69, respectively. Among the models considered herein, JMA and NCEP CFS best simulate the monsoon circulation over East Asia to the western Pacific. As will be made clear, a model's performance in simulating the mean monsoon strongly affects its ability to capture monsoon variability.

Table 2 Pattern correlations of mean 850 hPa wind and precipitation between observations and GCM simulations for the JJA season of 1983-2003, as shown in Fig. 3.

Models	U850	V850	PREC
BCC	0.57	0.15	-0.15
CWB	0.81	0.39	0.12
GCPS	0.83	0.50	0.57
GDAPS_F	0.79	0.35	0.23
JMA	0.93	0.71	0.78
MSC_GEM	0.55	0.32	0.58
MSC_GM2	0.79	0.44	0.69
MSC_GM3	0.86	0.62	0.76
MSC_SEF	0.88	0.54	0.15
NCEP	0.88	0.68	0.80
NIMR	0.58	0.02	0.54
PNU	0.83	0.59	0.69
POAMA	0.42	0.13	0.70

In order to examine the anomalous circulation associated with the variation of WNPSM activity in both model hindcasts and observational records, the JJA mean 850 hPa winds and precipitation are correlated with observations and are regressed onto the observed time series of the WNPMI. The latter is defined as the difference between the 850 hPa zonal wind averaged over the region of 5-15°N, 100-130°E, and that averaged over the more northern domain of 20-30°N, 110-140°E. The WNPMI

reflects the large-scale vorticity anomaly in the low-level monsoon flow, and is able to quantify the WNPSM variability in a concise manner (Wang et al., 2001). Figures 4 and 5 show the correlation maps of 850 hPa zonal wind and precipitation between the observations and the GCM simulations, respectively. The observed and simulated 850 hPa zonal winds are positively correlated along 10°N and 30°N in all of the models, and GCPS, GDAPS_F, JMA MSC_GM3 and NCEP show relatively strong correlations between the data sets in the defined two regions of the WNPMI (Fig. 4) GCPS, GDAPS, JMA, MSC_GM3 and NCEP show precipitation to be positively correlated in the region of 10-20°N, 120-170°N, which well corresponds to the regions of zonal circulation of the models (Fig. 5). The correlation patterns of zonal circulations in BCC, CWB, MSC_GEM, MSC_GM2, MSC_SEF, NIMR, PNU and POAMA are comparable, but their correlation patterns of precipitation are relatively weak and displaced in the western North Pacific.

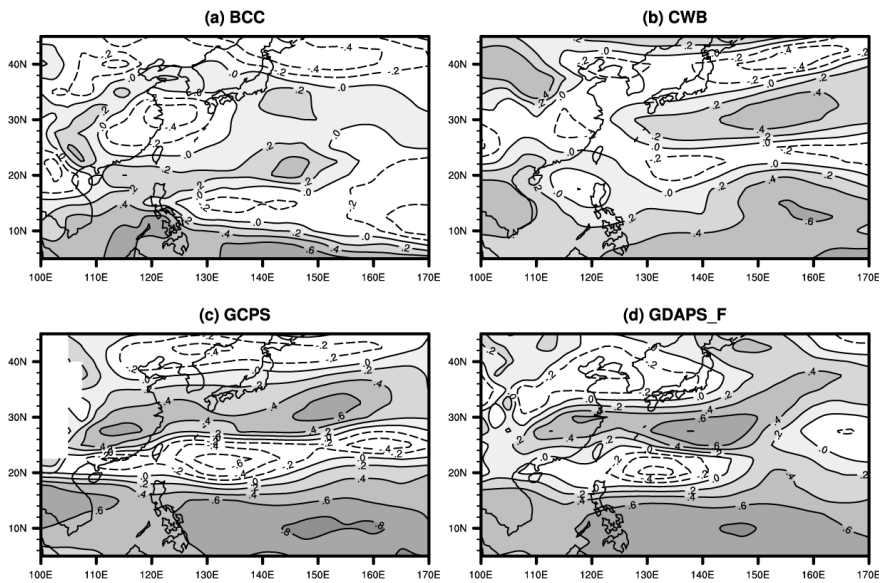

Figure 4 Correlation maps of 850 hPa zonal wind between observations and GCM simulations (a) BCC, (b) CWB, (c) GCPS, (d) GDAPS_F, (e) JMA, (f) MSC_GEM, (g) MSC_GM2, (h) MSC_GM3, (i) MSC_SEF, (j) NCEP, (k) NIMR, (l) PNU and (m) POAMA for the JJA season of 1983-2003.

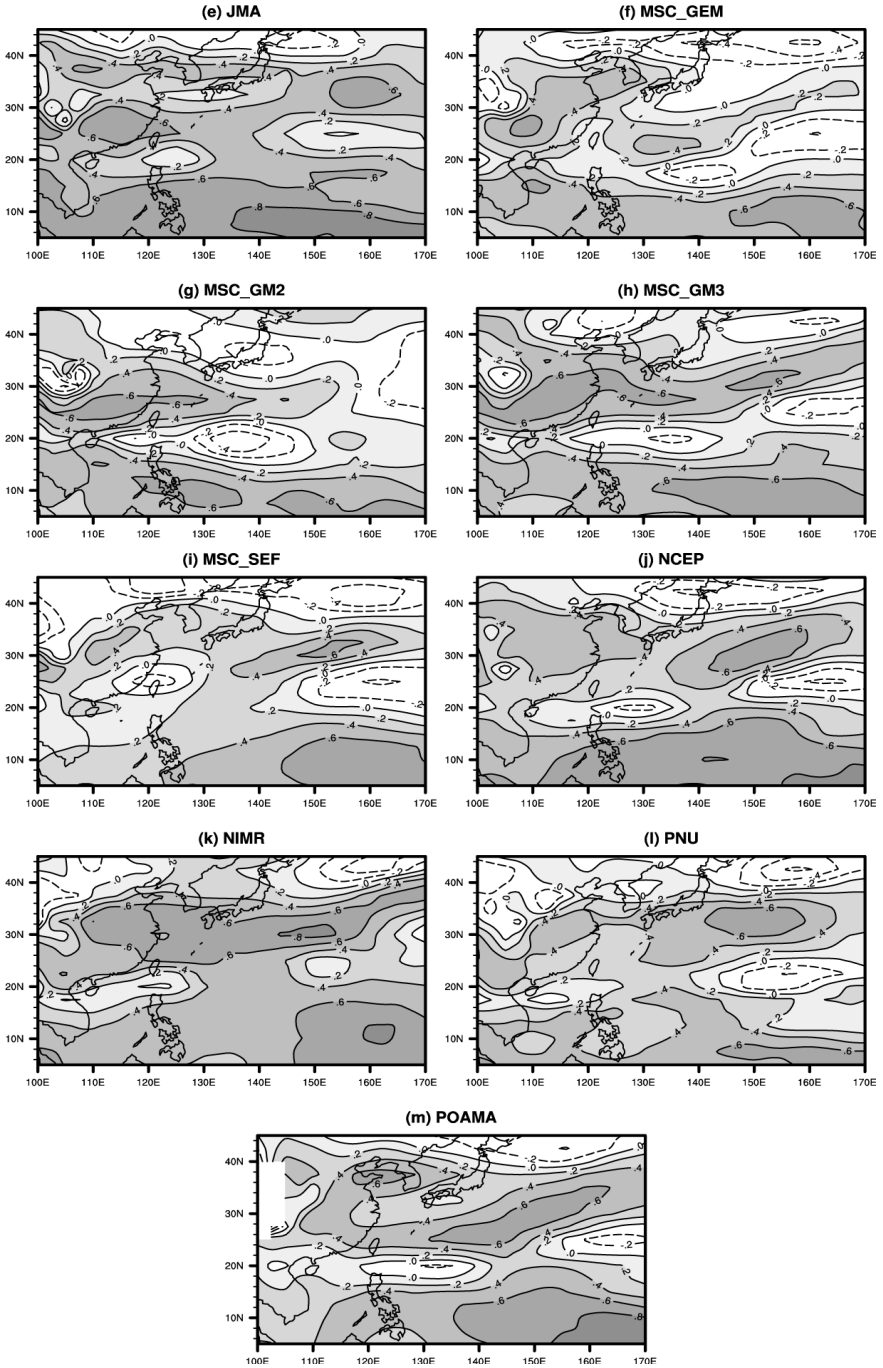

Figure 4 Continued.

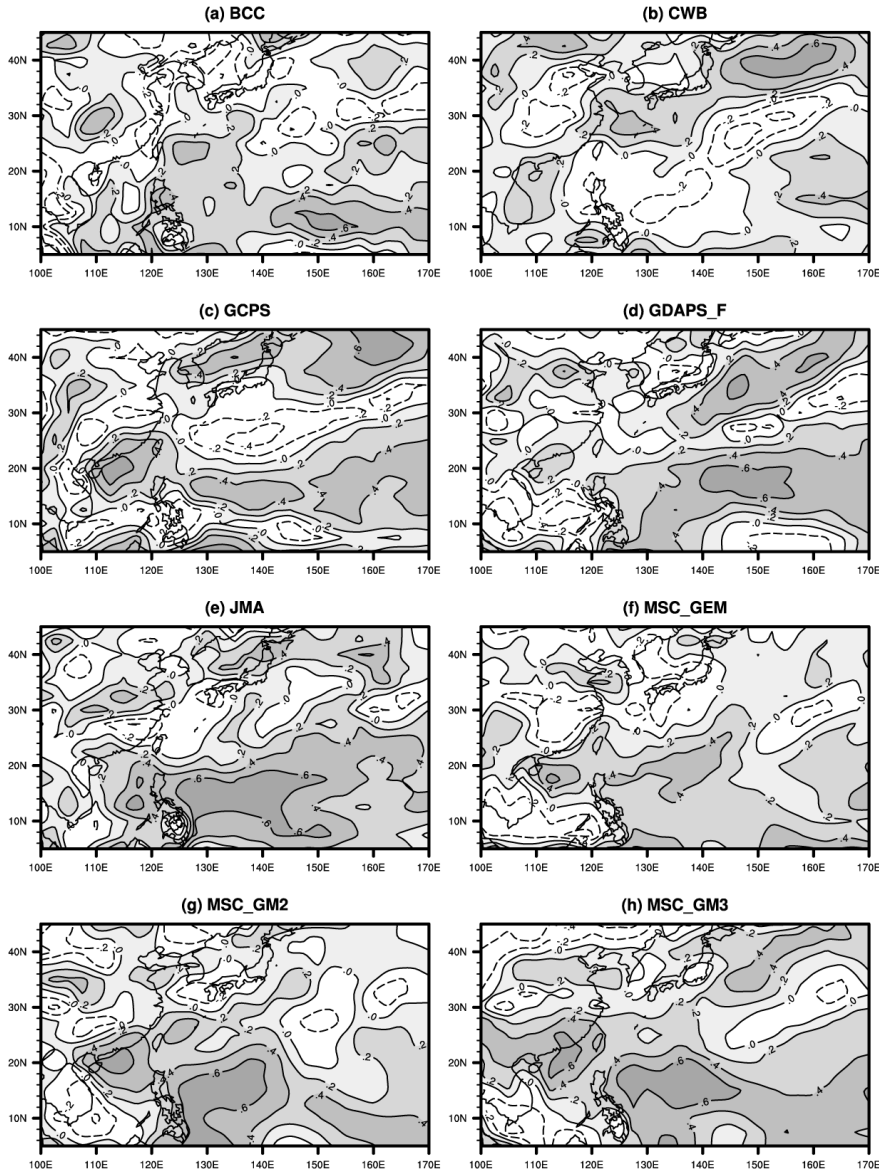

Figure 5 Correlation maps of precipitation between observations and GCM simulations (a) BCC, (b) CWB, (c) GCPS, (d) GDAPS_F, (e) JMA, (f) MSC_GEM, (g) MSC_GM2, (h) MSC_GM3, (i) MSC_SEF, (j) NCEP, (k) NIMR, (l) PNU and (m) POAMA for the JJA season of 1983-2003.

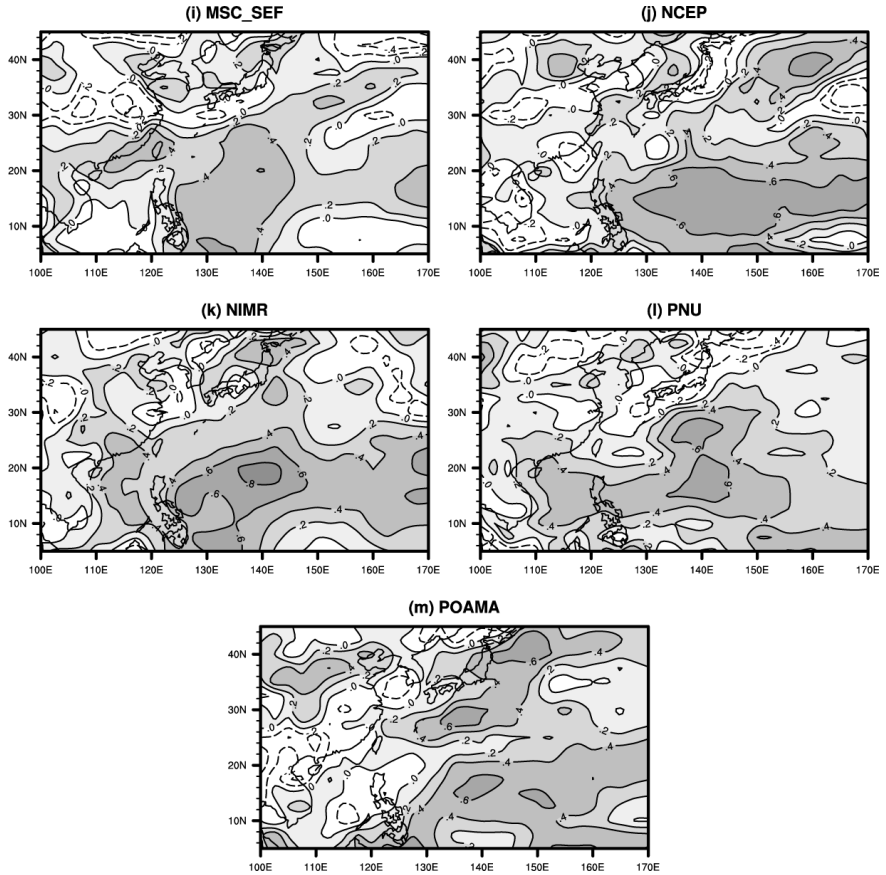

Figure 5 Continued.

3.2 WNPSM in observations, GCMs and MME onto the observed WNPMI

Figure 6 shows the results of the regression analysis based on observations as well as model hindcast simulations regressed onto the observed WNPMI. The observed WNPSM variability is characterized by an elongated low-level cyclone around 20°N that covers much of the subtropical western Pacific, the Philippines and the neighboring coastal regions (see Fig. 6a). Enhanced precipitation is present along the 5-20oN latitudinal band that covers the South China Sea, the Philippines and the western Pacific, over which strong westerly anomalies are found. In more northern locations around Japan and to its east, there is a prominent anticyclonic feature

associated with the WNPSM variability. Suppressed monsoon rainfall is found in the region and also over eastern China, indicating an out-of-phase relationship between the WNPSM and the Meiyu-Changma-Baiu rainfall.

Inspection of the 850 hPa wind simulation regression maps reveals cyclonic features over the subtropical western Pacific in most hindcast experiments, although the features are displaced in some model runs compared to observations (see Figs. 6c to 6o). This suggests that, to a certain extent, GCMs are able to reproduce large-scale circulation changes during years of strong WNPSM activity. However, many models struggle to accurately reproduce the precipitation pattern associated with WNPSM variability. CWB and GDAPS show rainfall anomalies over the Philippines with signs opposite those observed, and BCC and MSC_SEF show erroneous rainfall and circulation over the entire modeled region. The enhanced WNPSM rainfalls given by GCPS and POAMA are shifted 5-10o to the north and 10-20 o to the east of the observed rainfalls, respectively. JMA tends to show suppressed convection around the 20-25oN latitudinal band during strong WNPSM seasons, whereas observed rainfall tends to be lower further to the north. The rainfall patterns given by NCEP and NIMR are rather incoherent over the midlatitude region of East Asia. Interestingly, the variability patterns from some models are closely related to their mean circulation. For instance, in the CWB and GDAPS runs, suppressed (enhanced) precipitation over the more western (eastern) portion of East Asia and the western Pacific indicates that the models' monsoon rainfall is reinforced in its climatological mean locations during strong WNPSM years (see Fig. 6). Results from the GCPS run show a similar kind of reinforcement.

The same regression analysis is also carried out based on 850 hPa winds and rainfall from the MME mean hindcast data. Here, the MME mean is found by taking a simple (un-weighted) average of outputs from each model experiment. In contrast to those from individual model runs, wind and precipitation anomalies associated with the WNPSM variation are well reproduced in the MME mean hindcast (see Fig. 6b). There is enhanced (suppressed) rainfall at about 10oN (30oN), which is collocated with anomalous westerlies (easterlies) in the low levels over the western North Pacific. The MME result for precipitation is particularly remarkable given the

difficulty GCMs have in reproducing this pattern. Here it is worth noting that a common WNPMI time series is used in producing all the regression maps in Figure 6. Because an un-weighted average is taken in constructing the MME mean hindcast, the MME map is identical to the simple average of the regression maps from all models. Thus, the superior skill of MME can be attributed to the partial cancellation of model biases and mutual reinforcement of a more realistic prediction of the WNPSM. This is consistent with the notion that better sampling of errors from different models improves predictions in the MME approach.

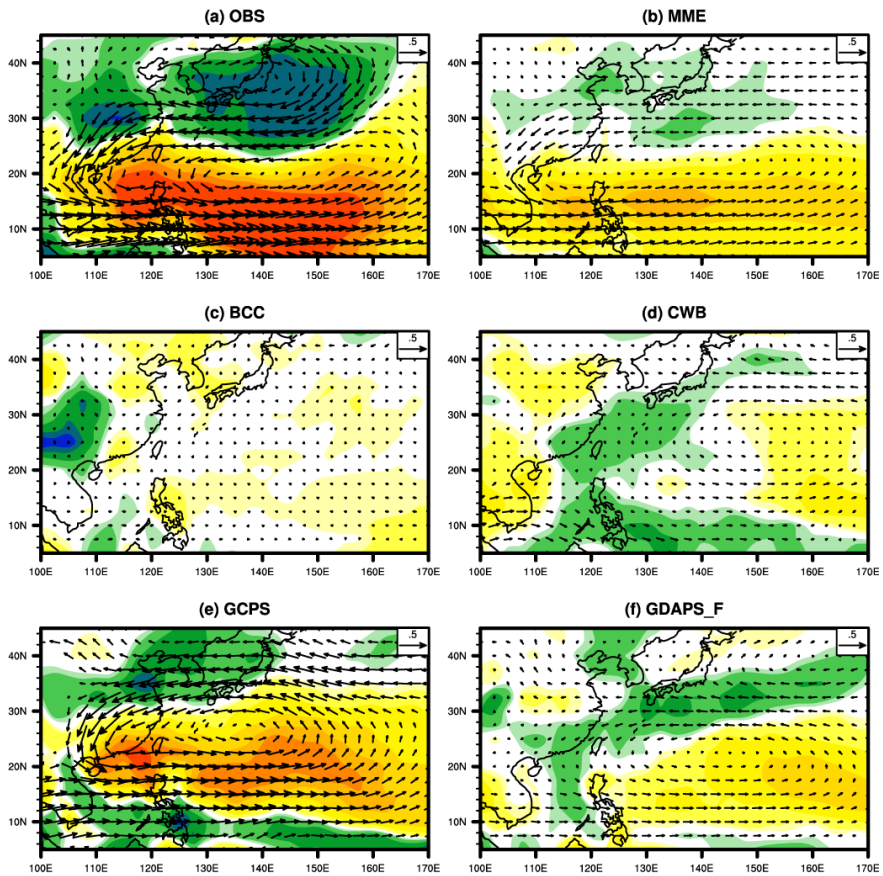

Figure 6 Regression maps of 850 hPa wind (vectors, see scale at upper right of each panel; units: ms^{-1}) and precipitation (shading, see scale bar at bottom; units: mm/day) based on (a) observations and (b) MME, (c) BCC, (d) CWB, (e) GCPS, (f) GDAPS_F, (g) JMA, (h) MSC_GEM, (i) MSC_GM2, (j) MSC_GM3, (k) MSC_SEF, (l) NCEP, (m) NIMR, (n) PNU and (o) POAMA simulations onto the observed WNPMI for the JJA season of 1983-2003.

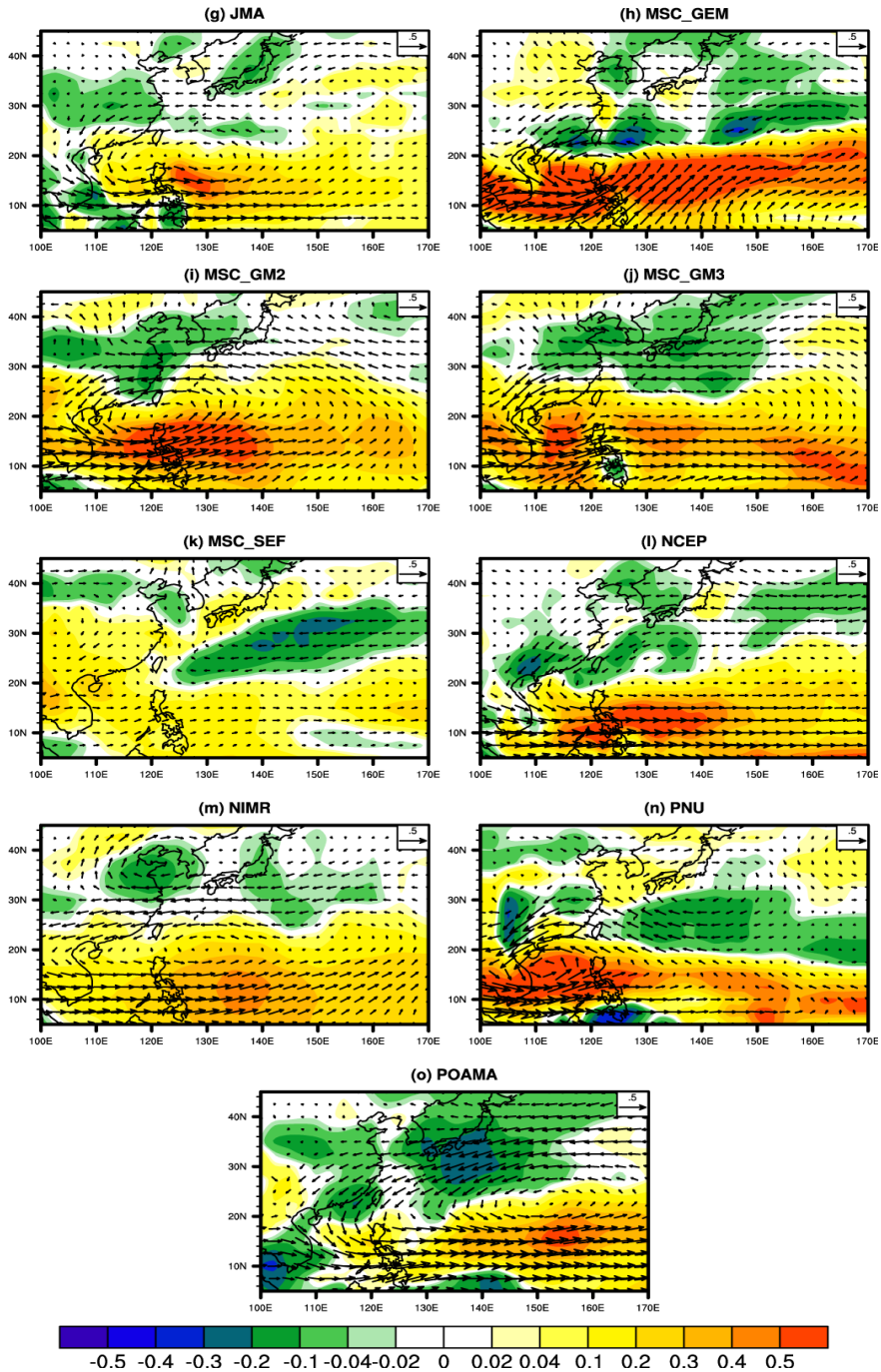

Figure 6 Continued.

3.3 Interannual variability of the WNPMI in observations, GCMs and MME

In addition to evaluating the circulation pattern of WNPSM variability, temporal variation in the model hindcast experiments is also examined. Figure 7 shows the observed WNPMI time series, as well as those from individual model outputs and the MME during the JJA season for the period of 1983-2003. The MME mean hindcast is seen to capture well the year-to-year variation of the WNPMI. The correlation between the MME result and observations is 0.73 during the hindcast period. This is consistent with the fact that the WNPSM circulation pattern in the MME well reflects its observational counterpart. On the other hand, the best individual model simulations by JMA and GDAPS_F give correlation values of 0.77 and 0.70, respectively. In summary, both the spatial and temporal variations of the WNPSM circulation are captured remarkably well in the MME mean retrospective predictions. We now investigate the WNPSM variability inherent in each dataset. Multivariate empirical orthogonal function (EOF) analysis is performed based on the u-wind and v-wind components averaged over the JJA period. Following Wang et al. (2001), the analysis domain is the western Pacific region of 5-45°N, 100-170°E. In observations, the leading EOF explains about 41% of the domain integrated variance of the winds, and its associated circulation anomalies, as revealed by regressing the 850 hPa wind and precipitation onto the first principal component (PC), are practically identical as those in Fig. 6a (figures not shown). This is because the WNPMI is highly correlated with the first PC with a correlation coefficient of 0.97, consistent with the results of Wang et al. (2001).

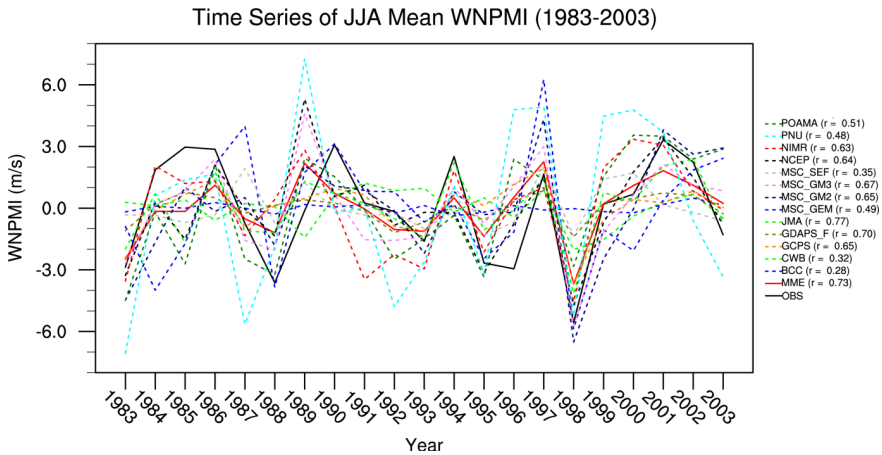

Figure 7 The WNPMI time series based on observations, individual model and MME hindcast for the JJA period from 1983 to 2003.

3.4 Model combinations of simple composite MMEs based on the leading WNPSM mode

The same EOF analysis is carried out for the hindcast runs from each individual model. Results are summarized in Table 3, which gives the pattern of correlation between the regression maps of circulation anomalies onto the leading PC from the model hindcasts, and those based on observations. Correlation values for the anomalous 850 hPa zonal wind and precipitation patterns are computed for the domain of 5-45°N, 100-170°E. Averaged over the results from each model, the mean pattern correlation coefficients for the 850 hPa zonal wind and precipitation are 0.67 and 0.44, respectively. The relatively low correlation in precipitation reflects the general difficulty GCMs have in capturing this field, consistent with the impression given by Fig. 6. In comparison, the MME mean data show considerably more realistic patterns of WNPSM variability; the pattern correlations between the MME data and observations are 0.91 and 0.71 for u-wind and precipitation, respectively. In summary, the MME approach is able to markedly improve the simulation of monsoon rainfall over the western Pacific relative to the performance achievable through a single model approach.

Table 3 Pattern correlations of 850 hPa zonal wind and precipitation between GCM simulations and observed circulation anomalies associated with the leading WNPSM mode for the JJA season of 1983-2003. The correlations with significance levels at 5% are shaded.

Models	U850	PREC
BCC	0.12	0.05
CWB	0.69	0.03
GCPS	0.62	0.26
GDAPS_F	0.60	0.36
JMA	0.86	0.73
MSC_GEM	0.90	0.56
MSC_GM2	0.82	0.32
MSC_GM3	0.79	0.33
MSC_SEF	0.05	0.37
NCEP	0.90	0.73
NIMR	0.69	0.77
PNU	0.80	0.57
POAMA	0.86	0.60
Model Ave.	0.67	0.44
MME	0.91	0.71

Based on the pattern correlations of both 850 hPa zonal wind and precipitation with significance levels at 5% given by Table 3 (shaded values), different simple composite MME model combinations are selected to examine their ability to predict the WNPSM (see Table 4). Most of the evaluated Tier-2 prediction systems (JMA, NCEP, PUN and POAMA) show high pattern correlations (more than 0.5) for both 850 hPa zonal wind and precipitation. As well, MSC_GEM and NIMR, which are Tier-1 systems, are seen to well reflect the leading WNPSM mode (more than 0.5 pattern correlations for both 850 hPa zonal wind and precipitation). Thus these four CGCMs and two AGCMs are selected as the top best model combinations (TMME). Other MME sets are grouped according to non-coupled (AMME) and coupled (CMME) prediction models. However, the models which give lower pattern correlations (BCC, CWB and MSC_SEF) are excepted from the CMME and AMME sets.

Table 4 Model sets of simple composite MMEs based on pattern correlations of 850 hPa zonal wind and precipitation between GCM simulations and observed circulation anomalies associated with the leading WNPSM mode for the JJA season of 1983-2003, as shown in Table 3. The models which have correlations significant at the 5% level for both 850 hPa zonal wind and precipitation are selected for three different simple composite MMEs, according to non-coupled (AMME), coupled (CMME) and the top best 6 models (TMME).

MMEs	Models					
MME	All models					
AMME (Tier-2)	GCPS	GDAPS_F	MSC_GEM	MSC_GM2	MSCGM3	NIMR
CMME (Tier-1)	JMA	NCEP	PNU	POAMA		
TMME (Top 6)	JMA	MSC_GEM	NCEP	NIMR	PNU	POAMA

3.5 Leading mode of the WNPSM interannual variability in simple composite MMEs

Figure 8 shows the regression of wind and precipitation on the leading PC based on the mean hindcasts of the four MMEs. The leading EOF of MME explains about 58% of the variance of the MME wind field. It is noteworthy that the circulation anomalies are also in good agreement with those of the observed data in Figure 6a. In other words, the leading mode of WNPSM wind variability in the MME hindcast well reflects its observational counterpart. The strong relationship between these WNPSM variability patterns explains why the MME low-level wind anomalies are well projected onto the regions used to define the WNPMI (see Fig. 6b). This relationship can be crucial in capturing the time variation of the WNPMI in the MME mean hindcast. In the case of other MMEs, the leading EOFs of AMME, CMME, and TMME explain about 56%, 68%, and 63% of the variances, respectively. The regression patterns of wind and precipitation from CMME and TMME are also comparable with those of the observed data shown in Figure 6a. In particular, the precipitation patterns of CMME and TMME are better reflective of the observations than MME and AMME, principally because the models are simple composites based on the patterns of precipitation from model hindcasts and observations projected onto the leading WNPSM mode. These results show that thoughtful model combination is critical to the performance of the MME approach.

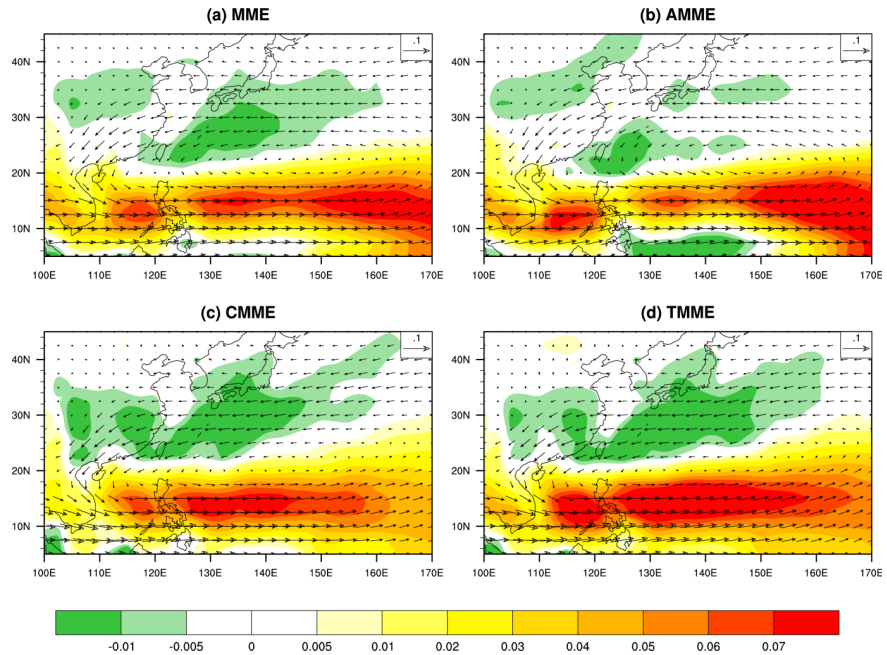

Figure 8 Regression coefficients of 850 hPa wind (vectors, see scale at upper right of each panel; units: ms^{-1}) and precipitation (shading, see scale bar at bottom; units: mm/day) onto the PC for leading WNPSM mode based on (a) MME, (b) AMME, (c) CMME and (d) TMME mean hindcasts.

3.6 Predictability of the WNPSM interannual variability in simple composite MMEs

We assess the role of the leading WNPSM mode in predicting the monsoon precipitation over the WNP region based on a comparison of MMEs and single models. The correlations between observed precipitation and mean precipitations from the four MMEs during the JJA season are computed for the 1983-2003 period. Figure 9 shows the correlation coefficients from the four MMEs mean hindcast precipitations as described in Table 4. The shaded areas are significant at the 5% level. In general, the WNPSM rainfalls simulated by single models are weakly correlated with observations, although the correlations of JMA and NCEP reach about 0.6 or more for the WNP region (10°-20°N, 130°-150°E) (see Fig. 5e, g, h, and j). On the other hand, the four MMEs mean hindcast precipitations are relatively well correlated with

observations over the WNPSM region (10°-20°N, 110°-150°E) (Fig. 9). In particular, the results of CMME and TMME are relatively well correlated with observed data compared to those of AMME. Interestingly, certain locations with enhanced correlations in the four MMEs, such as midlatitude East Asia, the western Pacific region and east of the Philippines, are largely coincident with areas where strong precipitation changes are associated with the leading WNPSM mode (see Fig. 6a). This highlights the importance of the WNPSM mode in determining monsoon predictability over the western North Pacific and parts of East Asia, and confirms that the MME method can substantially improve capture of this mode for the betterment of WMPSM rainfall prediction.

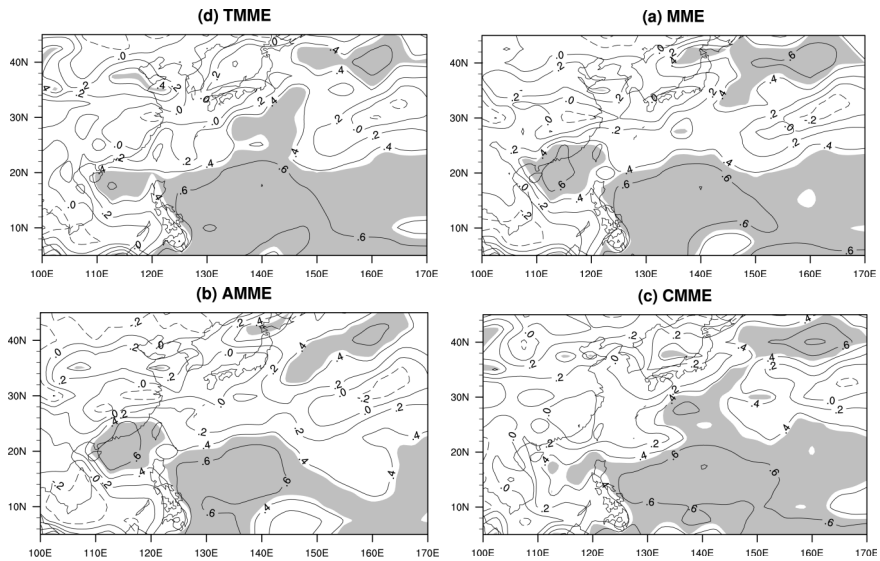

Figure 9 Correlation maps between observations and mean precipitation from (a) MME, (b) AMME, (c) CMME and (d) TMME for the JJA season of 1983-2003, as shown in Table 4.

We also assess the skill of four MMEs mean hindcast precipitations over the WNPSM and EASM regions. Figures 10 and 11 show the anomaly correlation coefficients of four MMEs mean hindcast precipitations over the WNPSM region (5°N-20°N, 100°E-150°E) and the EASM region (20°N-40°N, 100°E-140°E) during the JJA period of 1983-2003, respectively. The summer precipitation in the WNP-EA region

consists of a coupled tropical monsoon system related with cross-equatorial flows and the Australian High, and a subtropical monsoon system influenced by the WNP subtropical high and the EA subtropical monsoon front. As shown in Figure 3a, relatively strong precipitations occur over the Philippine Sea and its vicinity, and the South China Sea, Korea, and Japan, and are associated with the 'Meiyu', 'Baiu', and 'Changma'. Anomaly correlations of four MMEs over the WNPSM region, shown in Figure 10, show CMME to be most skillful among the MMEs for the period of record except for 1985 and 1986. Interestingly, CMME shows positive anomaly correlations in 1984, 1992, 1997, and 2003, whereas those of AMME are negative. This result implies that CGCMs can reproduce atmospheric circulation and precipitation over the WNPSM region, which is affected by surface temperature variations in the western Pacific that are linked to the ENSO. A comparison of the overall hindcast skill of the four MMEs over the two summer monsoon regions in Figures 10 and 11 shows it to be relatively lower over the EASM region than the WNPSM region. This disparity is principally attributable to the EASM being more significantly affected by continental land surface conditions and latitude conditions linked with the WNPSM. However, the four MMEs show good skill in many years, which means that both the WNPSM and EASM can be better predicted by a MME approach than by single model prediction.

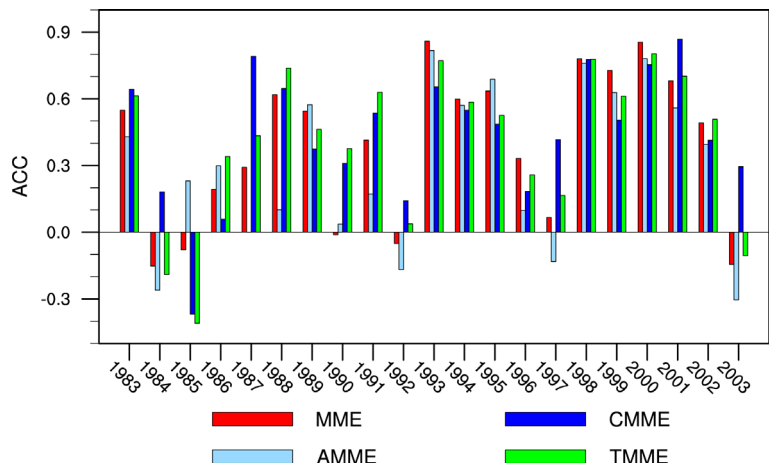

Figure 10 Anomaly correlation coefficients of four MMEs mean precipitations over the WNPSM region (5°N-20°N, 100°E-150°E) for the JJA period of 1983-2003.

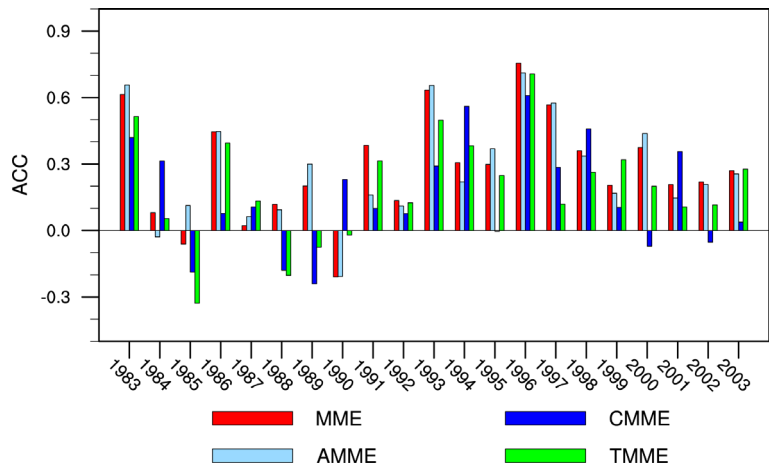

Figure 11 Anomaly correlation coefficients of four MMEs mean precipitations over the EASM region (20°N-40°N, 100°E-140°E) for the JJA period of 1983-2003.

4. CONCLUDING REMARKS

The interannual variability of the WNPSM has been assessed based on a set of retrospective predictions from thirteen GCMs participating in the APCC MME seasonal forecasts. It is found that the mean hindcasts of four MMEs can reliably reproduce changes in both low-level wind and precipitation during years of strong WNPSM variations. The observed cyclonic flow anomalies in the western Pacific as well as enhanced (reduced) precipitation near the Philippines (subtropical to midlatitude East Asia) are well represented in the mean results of the four MMEs. In contrast, the single-model simulations poorly reflect the typical changes in WNPSM circulation, especially those in the precipitation field. The year-to-year evolution of the WNPSM is also well predicted by the mean results of the MMEs, which give better performance than each of the individual models. The leading mode of WNPSM low-level wind variability from the MMEs mean hindcast is also shown to well reflect observations. Overall, the MME approach considerably improves monsoon rainfall prediction over the western North Pacific domain relative to single model approaches. The relative good performance of the MME forecast can be attributed to better

quantification of uncertainty due to the cancelation of biases inherent to each model: in general, better sampling in the multi-model method leads to partial cancellation of model errors and reinforcement of more realistic simulations in the MME mean prediction.

Based on the model runs examined here, low-level winds are found to be better simulated, relative to rainfall, over the WNPSM region. This is true for both single-model and MME predictions (see Table 3). In principle, the ability of GCMs to capture large-scale circulation variables can be harnessed to improve summer monsoon rainfall forecasts through statistical post-processing. Recent studies on statistical downscaling of MME products show that this method is promising even for station-scale rainfall predictions (Kang et al., 2007; Chu et al., 2008).

Finally, our results highlight the importance of air-sea coupling on WNPSM variability simulation. Wang et al. (2005), based on multi-model integrations with observed SST, found WNPSM variability to be poorly reflected in their MME average results. Here, however, the MME hindcast can reproduce both the spatial and temporal variations of the WNPSM. In fact, besides CMME, which includes Tier-1 systems, TMME is also found to accurately capture WNPSM variability (see Fig. 9 and Fig. 10). The latter prediction system employs the best atmospheric GCMs and CGCMs with either persistent or predicted SST anomalies prescribed in their hindcast experiments. Therefore, it seems that model choice is also crucial in determining the success of the MME approach in predicting monsoon variability. Further studies are needed to elucidate in detail the relative roles of air-sea interaction and model physics in dynamical monsoon prediction.

REFERENCES

Barnston, A. G., S. J. Mason, L. Goddard, D. G. Dewitt, and S. E. Zebiak, 2003: Multimodel ensembling in seasonal climate forecasting at IRI. *Bull. Amer. Am. Meteor. Soc., 84*, 1783-1796.

Chang, C.-P., Y. Zhang, and T. Li, 2000: Interannual and interdecadal variations of the East Asian summer monsoon and tropical Pacific SSTs. Part I: Roles of the subtropical ridge. *J. Climate*, 13, 4310-4325.

Chou, C., J. Tu, and J. Yu, 2003: Interannual Variability of the Western North Pacific Summer Monsoon: Differences between ENSO and Non-ENSO Years. *J. Climate*, 16, 2275-2287.

Chu, J.-L., H. Kang, C.-Y. Tam, C.-K. Park and C.-T. Chen, 2008: Seasonal forecast for local precipitation over northern Taiwan using statistical downscaling. *J. Geophys. Res.*, in press.

Janowiak, J. E. and P. Xie, 1999: CAMS_OPI: A global satellite-raingauge merged product for real-time precipitation monitoring applications. *J. Climate*, 12, 3335-3342.

Kanamitsu, M., and co-authors (2002), NCEP-DOE AMIP-II Reanalysis (R-2), *Bull. Amer. Meteor. Soc.* 83, 1631-1643.

Kang, H., K.-H. An, C.-K. Park, A. L. S. Solis, and K. Stitthichivapak, 2007: Multi-model output statistical downscaling prediction of precipitation in the Philippines and Thailand, *Geophys. Res. Lett., 34*, L15710, doi:10.1029/2007GL030730.

Kang, I.-S. and J. Shukla, 2005: Dynamical seasonal prediction and predictability of monsoon, *The global monsoon system: research and forecast, Report of the International Committee of the third international workshop on monsoons (IWM-III), WMO/TD No. 1266*, 386-402.

Kang, I.-S., K. Jin, B. Wang, K.-M. Lau, J. Shukla, V. Krishnamurthy, S. D. Schubert, D. E. Wailser, W. F. Stern, A. Kitoh, G. A. Meehl, M. Kanamitsu, V. Y. Galin, V. Satyan, C.-K. Park, and Y. Liu, 2002: Intercomparison of the climatological variations of Asian summer monsoon precipitation simulated by 10 GCMs. *Clim.ate Dyn., 19*, 383-395.

Krishnamurti, T. N., C. M. Kishtawal, Z. Zhang, T. E. LaRow, D. R. Bachiochi, C. E. Williford, S. Gadgil, and S. Surendran, 2000: Multi-model ensemble forecasts for weather and seasonal climate. *J. Climate*, 13, 4196-4216.

Palmer, T. N., A. Alessandri, U. Andersen, P. Cantelaube, M. Davey , P. Délécluse, M. Déqué, E. Diez, F. J. Doblas-Reyes, H. Feddersen, R. Graham, S. Gualdi, J.-F. Guérémy, R. Hagedorn, M. Hoshen, N. Keenlyside, M. Latif, A. Lazar, E. Maisonnave, V. Marletto, A. P. Morse, B. Orfila, P. Rogel, J.-M. Terres, and M. C. Thomson, 2004: Development of a European multimodel ensemble system for seasonal-to-interannual prediction (DEMETER). *Bull. Am.Amer. Meteor. Soc., 85*, 853–872.

Sumi, A., N.-C. Lau, and W.-C. Wang, 2005: Present status of Asian monsoon simulation. *The global monsoon system: research and forecast, Report of the International Committee of the third international workshop on monsoons (IWM-III), WMO/TD No. 1266*, 376-385.

Tanaka, M., 1997: Interannual and interdecadal variations of the western North Pacific monsoon and the East Asian Baiu rainfall and their relationship to ENSO cycles. *J. Meteor. Soc. Japan*, 75, 1109-1123.

Wang, B., and Z. Fan, 1999: Choice of South Asia summer monsoon indices. *Bull. Amer. Meteo. Soc.*, 80, 629-638.

Wang, B., I.-S. Kang, and J.-Y. Lee, 2004: Ensemble simulations of Asian-Australian Monsoon Variability by 11 AGCMs. *J. Climate*, 17, 803-818.

Wang, B., J.-Y. Lee, I.-S. Kang, J. Shukla et al., 2008: Assessment of the APCC/CliPAS 14-Model Ensemble Retrospective Seasonal Prediction (1980–2004). *Climate Dyn.* in press.

Wang, B., Q. Ding, X. Fu, I.-S. Kang, K. Jin, J. Shukla and F. Doblas-Reyes, 2005: Fundamental challenge in simulation and prediction of summer monsoon rainfall. *Geophys. Res. Lett., 32*, L15711, doi:10.1029/2005GL022734.

Wang, B., R. Wu, and K.-M. Lau, 2001: Interannual variability of the Asian summer monsoon: contrasts between the Indian and the western North Pacific-East Asian monsoons. *J. Climate, 14*, 4073-4090.

Wang, B., R. Wu, and R. Lukas, 1999: Roles of the western North Pacific wind variation in thermocline adjustment and ENSO phase transition. *J. Meteor. Soc. Japan*, 77, 1-16.

Wang, B., R. Wu, and X. Fu, 2000: Pacific-East Asia teleconnection: How does ENSO affect East Asian climate? *J. Climate*, 13, 1517-1536.

Wu, R., and B. Wang, 2000: Interannual variability of summer monsoon onset over the Western North Pacific and underlying processes. *J. Climate*, 13, 2483-2501.

Yasunari, T., 1990: Impact of Indian monsoon on the coupled atmosphere/ocean system in the tropical Pacific. *Meteor. Atmos. Phys.*, 44, 29-41.

APCC TECHNICAL REPORT 2011-01

- Interannual Variability of the Western North Pacific Summer Monsoon
- Reduction Biases in Regional Climate Downscaling
- Typhoon Activity in the North West Pacific Region

APEC Climate Center

12, Centum 7-ro, Haeundae-gu, Busan 612-020,
Republic of Korea
Tel: +82-51-745-3900 Fax: +82-51-745-3949
www.apcc21.org

비매품
94500
9 788997 533165
ISBN 978-89-97333-16-5
ISBN 978-89-97333-15-8 (세트)